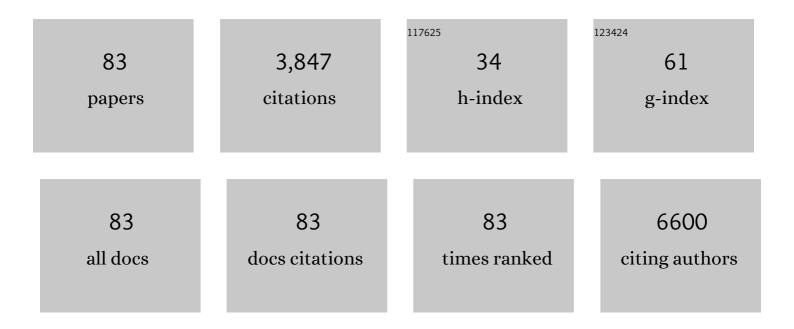
List of Publications by Year in descending order

Source: https://exaly.com/author-pdf/10513989/publications.pdf Version: 2024-02-01



ROCEP K LAKE

#	Article	IF	CITATIONS
1	Tin Disulfide—An Emerging Layered Metal Dichalcogenide Semiconductor: Materials Properties and Device Characteristics. ACS Nano, 2014, 8, 10743-10755.	14.6	449
2	Electronic and thermoelectric properties of few-layer transition metal dichalcogenides. Journal of Chemical Physics, 2014, 140, 124710.	3.0	321
3	Thermal Percolation Threshold and Thermal Properties of Composites with High Loading of Graphene and Boron Nitride Fillers. ACS Applied Materials & Interfaces, 2018, 10, 37555-37565.	8.0	243
4	A charge-density-wave oscillator based on an integrated tantalum disulfide–boron nitride–graphene device operating at room temperature. Nature Nanotechnology, 2016, 11, 845-850.	31.5	170
5	Monolayer \$hbox{MoS}_{2} Transistors Beyond the Technology Road Map. IEEE Transactions on Electron Devices, 2012, 59, 3250-3254.	3.0	156
6	Charge Density Waves in Exfoliated Films of van der Waals Materials: Evolution of Raman Spectrum in TiSe ₂ . Nano Letters, 2012, 12, 5941-5945.	9.1	154
7	Quantitative simulation of a resonant tunneling diode. Journal of Applied Physics, 1997, 81, 3207-3213.	2.5	139
8	Electronic and thermoelectric properties of van der Waals materials with ring-shaped valence bands. Journal of Applied Physics, 2015, 118, .	2.5	120
9	Fundamentals of lateral and vertical heterojunctions of atomically thin materials. Nanoscale, 2016, 8, 3870-3887.	5.6	117
10	Towards van der Waals Epitaxial Growth of GaAs on Si using a Graphene Buffer Layer. Advanced Functional Materials, 2014, 24, 6629-6638.	14.9	113
11	Direct Bandgap Transition in Many‣ayer MoS ₂ by Plasmaâ€Induced Layer Decoupling. Advanced Materials, 2015, 27, 1573-1578.	21.0	102
12	Hot carrier-enhanced interlayer electron–hole pair multiplication in 2D semiconductor heterostructure photocells. Nature Nanotechnology, 2017, 12, 1134-1139.	31.5	74
13	Direct observation of confined acoustic phonon polarization branches in free-standing semiconductor nanowires. Nature Communications, 2016, 7, 13400.	12.8	71
14	Long-distance spin transport through a graphene quantum Hall antiferromagnet. Nature Physics, 2018, 14, 907-911.	16.7	70
15	Graphene-based non-Boolean logic circuits. Journal of Applied Physics, 2013, 114, .	2.5	60
16	Phonon and Thermal Properties of Quasi-Two-Dimensional FePS ₃ and MnPS ₃ Antiferromagnetic Semiconductors. ACS Nano, 2020, 14, 2424-2435.	14.6	58
17	Bias-Voltage Driven Switching of the Charge-Density-Wave and Normal Metallic Phases in 1T-TaS ₂ Thin-Film Devices. ACS Nano, 2019, 13, 7231-7240.	14.6	57
18	Transmission resonances and zeros in multiband models. Physical Review B, 1995, 52, 2754-2765.	3.2	56

#	Article	IF	CITATIONS
19	A brain-plausible neuromorphic on-the-fly learning system implemented with magnetic domain wall analog memristors. Science Advances, 2019, 5, eaau8170.	10.3	56
20	Effects of band-tails on the subthreshold characteristics of nanowire band-to-band tunneling transistors. Journal of Applied Physics, 2011, 110, .	2.5	54
21	Topological spin Hall effect resulting from magnetic skyrmions. Physical Review B, 2015, 92, .	3.2	53
22	Negative differential resistance in bilayer graphene nanoribbons. Applied Physics Letters, 2011, 98, .	3.3	52
23	Phase Engineering of 2D Tin Sulfides. Small, 2016, 12, 2998-3004.	10.0	51
24	Raman spectra of twisted CVD bilayer graphene. Carbon, 2017, 123, 302-306.	10.3	50
25	One-dimensional van der Waals quantum materials. Materials Today, 2022, 55, 74-91.	14.2	49
26	Performance of \$n\$-Type InSb and InAs Nanowire Field-Effect Transistors. IEEE Transactions on Electron Devices, 2008, 55, 2939-2945.	3.0	48
27	Leakage and performance of zero-Schottky-barrier carbon nanotube transistors. Journal of Applied Physics, 2005, 98, 064307.	2.5	44
28	Material Selection for Minimizing Direct Tunneling in Nanowire Transistors. IEEE Transactions on Electron Devices, 2012, 59, 2064-2069.	3.0	41
29	Permanent Electric Dipole Moments of Carboxyamides in Condensed Media: What Are the Limitations of Theory and Experiment?. Journal of Physical Chemistry B, 2011, 115, 9473-9490.	2.6	39
30	Skyrmion creation and annihilation by spin waves. Applied Physics Letters, 2015, 107, .	3.3	39
31	Commensurate lattice constant dependent thermal conductivity of misoriented bilayer graphene. Carbon, 2018, 138, 451-457.	10.3	38
32	Conductance switching in diarylethenes bridging carbon nanotubes. Journal of Chemical Physics, 2011, 134, 024524.	3.0	37
33	Electron transport through a conjugated molecule with carbon nanotube leads. Physical Review B, 2007, 76, .	3.2	35
34	Acoustic phonon spectrum and thermal transport in nanoporous alumina arrays. Applied Physics Letters, 2015, 107, .	3.3	35
35	Drive Currents and Leakage Currents in InSb and InAs Nanowire and Carbon Nanotube Band-to-Band Tunneling FETs. IEEE Electron Device Letters, 2009, 30, 1257-1259.	3.9	31
36	The coherent interlayer resistance of a single, rotated interface between two stacks of AB graphite. Applied Physics Letters, 2013, 103, 243114.	3.3	25

#	Article	IF	CITATIONS
37	Theoretical and experimental study of highly textured GaAs on silicon using a graphene buffer layer. Journal of Crystal Growth, 2015, 425, 268-273.	1.5	25
38	Diameter dependent performance of high-speed, low-power InAs nanowire field-effect transistors. Journal of Applied Physics, 2010, 107, 014502.	2.5	24
39	Uniform Benchmarking of Low-Voltage van der Waals FETs. IEEE Journal on Exploratory Solid-State Computational Devices and Circuits, 2016, 2, 28-35.	1.5	24
40	The Quantum and Classical Capacitance Limits of InSb and InAs Nanowire FETs. IEEE Transactions on Electron Devices, 2009, 56, 2215-2223.	3.0	23
41	Theoretical design of bioinspired macromolecular electrets based on anthranilamide derivatives. Biotechnology Progress, 2009, 25, 915-922.	2.6	23
42	Two step growth phenomena of molybdenum disulfide–tungsten disulfide heterostructures. Chemical Communications, 2015, 51, 11213-11216.	4.1	21
43	Conductance of a conjugated molecule with carbon nanotube contacts. Physical Review B, 2009, 80, .	3.2	20
44	Growth Dynamics of Millimeterâ€sized Singleâ€Crystal Hexagonal Boron Nitride Monolayers on Secondary Recrystallized Ni (100) Substrates. Advanced Materials Interfaces, 2019, 6, 1901198.	3.7	20
45	Strain control of the Néel vector in Mn-based antiferromagnets. Applied Physics Letters, 2019, 114, .	3.3	20
46	Effect of Random, Discrete Source Dopant Distributions on Nanowire Tunnel FETs. IEEE Transactions on Electron Devices, 2014, 61, 2208-2214.	3.0	19
47	Shape dependent resonant modes of skyrmions in magnetic nanodisks. Journal of Magnetism and Magnetic Materials, 2018, 455, 9-13.	2.3	19
48	Room-Temperature Electrodeposition of Aluminum via Manipulating Coordination Structure in AlCl3 Solutions. Journal of Physical Chemistry Letters, 2020, 11, 1589-1593.	4.6	18
49	Carbon nanotube - molecular resonant tunneling diode. Physica Status Solidi (A) Applications and Materials Science, 2006, 203, R5-R7.	1.8	17
50	Doping, Tunnel Barriers, and Cold Carriers in InAs and InSb Nanowire Tunnel Transistors. IEEE Transactions on Electron Devices, 2012, 59, 2996-3001.	3.0	17
51	Current modulation by voltage control of the quantum phase in crossed graphene nanoribbons. Physical Review B, 2012, 86, .	3.2	16
52	High-frequency current oscillations in charge-density-wave 1T-TaS2 devices: Revisiting the "narrow band noise―concept. Applied Physics Letters, 2020, 116, .	3.3	15
53	Modeling and performance analysis of GaN nanowire field-effect transistors and band-to-band tunneling field-effect transistors. Journal of Applied Physics, 2010, 108, 104503.	2.5	13
54	Core size dependence of the confinement energies, barrier heights, and hole lifetimes in Ge-core/Si-shell nanocrystals. Journal of Applied Physics, 2011, 110, .	2.5	13

#	Article	IF	CITATIONS
55	Hybrid Graphene Nanoribbon-CMOS tunneling volatile memory fabric. , 2011, , .		12
56	Strong Circularly Polarized Photoluminescence from Multilayer MoS ₂ Through Plasma Driven Direct-Gap Transition. ACS Photonics, 2016, 3, 310-314.	6.6	12
57	Interlayer transport through a graphene/rotated boron nitride/graphene heterostructure. Physical Review B, 2017, 95, .	3.2	12
58	Interlayer resistance of misoriented MoS ₂ . Physical Chemistry Chemical Physics, 2017, 19, 10406-10412.	2.8	12
59	Phononic and photonic properties of shape-engineered silicon nanoscale pillar arrays. Nanotechnology, 2020, 31, 30LT01.	2.6	12
60	Electronic properties of carbon nanotubes calculated from density functional theory and the empirical I€-bond model. Journal of Computational Electronics, 2007, 6, 395-400.	2.5	11
61	<pre>\$hbox{TiSi}_{2}\$ Nanocrystal Metal Oxide Semiconductor Field Effect Transistor Memory. IEEE Nanotechnology Magazine, 2011, 10, 499-505.</pre>	2.0	10
62	Metallic <i>vs.</i> semiconducting properties of quasi-one-dimensional tantalum selenide van der Waals nanoribbons. Nanoscale, 2022, 14, 6133-6143.	5.6	10
63	Performance analysis of InP nanowire band-to-band tunneling field-effect transistors. Applied Physics Letters, 2009, 95, 073504.	3.3	9
64	Spin-Josephson effects in exchange coupled antiferromagnetic insulators. Physical Review B, 2016, 94, .	3.2	9
65	Nanoscale phononic interconnects in THz frequencies. Physical Chemistry Chemical Physics, 2014, 16, 23355-23364.	2.8	8
66	Electron transport through antiferromagnetic spin textures and skyrmions in a magnetic tunnel junction. Physical Review B, 2020, 102, .	3.2	7
67	Growth of High-Quality Hexagonal Boron Nitride Single-Layer Films on Carburized Ni Substrates for Metal–Insulator–Metal Tunneling Devices. ACS Applied Materials & Interfaces, 2020, 12, 35318-35327.	8.0	7
68	Effects of filling, strain, and electric field on the Néel vector in antiferromagnetic CrSb. Physical Review B, 2020, 102, .	3.2	7
69	Self-Assembled Carbon Nanotubes for Electronic Circuit and Device Applications. Journal of Nanoelectronics and Optoelectronics, 2006, 1, 74-81.	0.5	7
70	Tunneling spectroscopy of chiral states in ultra-thin topological insulators. Journal of Applied Physics, 2013, 113, 063707.	2.5	6
71	Vibronic Exciton–Phonon States in Stack-Engineered van der Waals Heterojunction Photodiodes. Nano Letters, 2022, 22, 5751-5758.	9.1	6
72	The quantum capacitance limit of high-speed, low-power InSb nanowire field effect transistors. , 2008, , .		5

#	Article	IF	CITATIONS
73	Electronic states of Ge/Si nanocrystals with crescent-shaped Ge-cores. Journal of Applied Physics, 2012, 112, .	2.5	5
74	Interlayer magnetoconductance of misoriented bilayer graphene ribbons. Journal of Applied Physics, 2013, 114, .	2.5	5
75	Multi-state current switching by voltage controlled coupling of crossed graphene nanoribbons. Journal of Applied Physics, 2013, 114, 153710.	2.5	5
76	Effect of strain on the electronic and optical properties of Ge–Si dome shaped nanocrystals. Physical Chemistry Chemical Physics, 2015, 17, 2484-2493.	2.8	5
77	Synthetic antiferromagnet-based spin Josephson oscillator. Applied Physics Letters, 2020, 116, 132409.	3.3	5
78	Carrier leakage in Ge/Si core-shell nanocrystals for lasers: core size and strain effects. Proceedings of SPIE, 2011, , .	0.8	3
79	Interface effects in tunneling models with identical real and complex dispersions. Physical Review B, 1999, 59, 7316-7319.	3.2	1
80	Effects of heavily doped source on the subthreshold characteristics of nanowire tunneling transistors. , 2011, , .		1
81	Tuning Spin Transport in a Graphene Antiferromagnetic Insulator. Physical Review Applied, 2022, 18, .	3.8	1
82	High-Speed and Low-Power Performance of n-type InSb/InP and InAs/InP Core/Shell Nanowire Field Effect Transistors for CMOS Logic Applications. Materials Research Society Symposia Proceedings, 2009, 1178, 26.	0.1	0
83	Modeling and performance analysis of high-speed, high-power GaN nanowire FETs. , 2009, , .		0